ACS APPLIED MATERIALS & INTERFACES

Research Article

www.acsami.org

Opportunities with Fabric Composites as Unique Flexible Substrates

Samuel A. Pendergraph, Michael D. Bartlett, Kenneth R. Carter,* and Alfred J. Crosby*

Department of Polymer Science and Engineering, University of Massachusetts, 120 Governors Dr. Amherst, Massachusetts 01003-9265, United States

Supporting Information

ABSTRACT: Flexible substrates enable new capabilities in applications ranging from electronics to biomedical devices. To provide a new platform for these applications, we investigate a composite material consisting of rigid fiber fabrics impregnated with soft elastomers, offering the ability to create load bearing, yet flexible substrates. We demonstrate an integrated and facile one-step imprint lithographic patterning method on a number of fabrics and resins. Furthermore, the bending and tensile properties were examined to compare the composites to other flexible materials such as PET and cellulose paper. Carbon fiber composites possess a higher tensile modulus than PET while retaining almost an order of magnitude lower bending modulus. Fabric composites can also have anisotropic mechanical properties not observed in homogeneous materials. Finally, we provide a discussion of these anisotropic mechanical responses and their potential use in flexible applications.

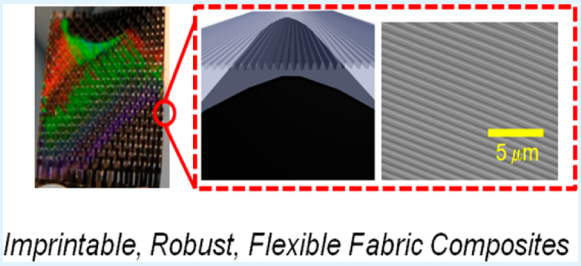

KEYWORDS: *lithography, substrate, flexible, mechanics*

INTRODUCTION

Flexible materials are currently in strong demand for a number of applications, such as flexible electronics and biomedical devices, which require conformability to surfaces and stability under large deformations.[1−5] In order to satisfy this challenge, many flexible substrates tend to be very thin to reduce the strain induced by bending.[6−8] Poly (ethylene terepthalate) (PET)[6,9−12] and poly(ethylene napthalate) (PEN)[10,13] have been studied extensively because of their toughness and transparency. Although PET and PEN have attractive qualities, there are difficulties with coating these materials, such as delamination and dewetting.[10] Another approach used to achieve large bending deformations for a flexible substrate is to use low modulus materials. Silicone rubber compositions based upon cross-linked poly(dimethylsiloxane), such as Sylgard 184, (referred to as x-PDMS in this paper) have been demonstrated in flexible substrate applications because of its ability to undergo large and reversible strains and its high bending flexibility.[14−18] Rogers and co-workers have elegantly demonstrated that under appropriate geometric parameters and processing techniques, x-PDMS can be a versatile platform for flexible electronics.[19−25] Despite the attractive features of x-PDMS compositions, they have a much lower elastic modulus than that of PET or PEN, which may be limiting in certain applications where high mechanical loads are necessary.[14,15]

To take advantage of both a load-bearing material, such as PET or PEN, and the low modulus of silicone rubbers, researchers have integrated stiff materials with soft elastomeric gels. Materials such as paper[26−31] or leather and latex[32] embedded in x-PDMS, as well as gels consisting of ionic liquid and single-wall carbon nanotubes[33] have been used as flexible supports. Moreover, nonwoven and woven fiber fabrics have also been investigated as flexible substrates. Bae and co-workers have demonstrated the use of a robust woven glass fiber−composite system as a flexible and transparent substrate for transistors and solar cells.[34] However, all the aforementioned findings focus on the device fabrication and lack measurement on the mechanical properties of the substrate. Furthermore, these reports discuss a two-step patterning approach that involves evaporation or printing of materials onto the substrate rather than directly patterning the substrate material.

In this work, we evaluate the mechanical properties of fabric composites which can serve as an alternative for flexible, patterned substrates. In contrast to much of the previous work where substrates were designed to be either flexible or flexible and stretchable, we investigate substrates with remarkable flexibility as well as high in-plane stiffness, a unique combination of properties that has not been largely investigated. Further, we demonstrate a one-step imprint lithographic procedure to form patterned composites which easily bend but possess high tensile stiffness. Patterned fabric composites are shown to withstand rapid cyclic loading without noticeable degradation of the features. By changing the combination of fabric and resin systems, we demonstrate tunable mechanical properties including high load bearing capacity while maintaining a lower bending modulus. Through this evaluation, these unique properties are discussed in order to provide new, flexible substrate for various applications.

Received: August 24, 2012
Accepted: November 13, 2012
Published: November 13, 2012

   dx.doi.org/10.1021/am3017812 | *ACS Appl. Mater. Interfaces* 2012, 4, 6640−6645

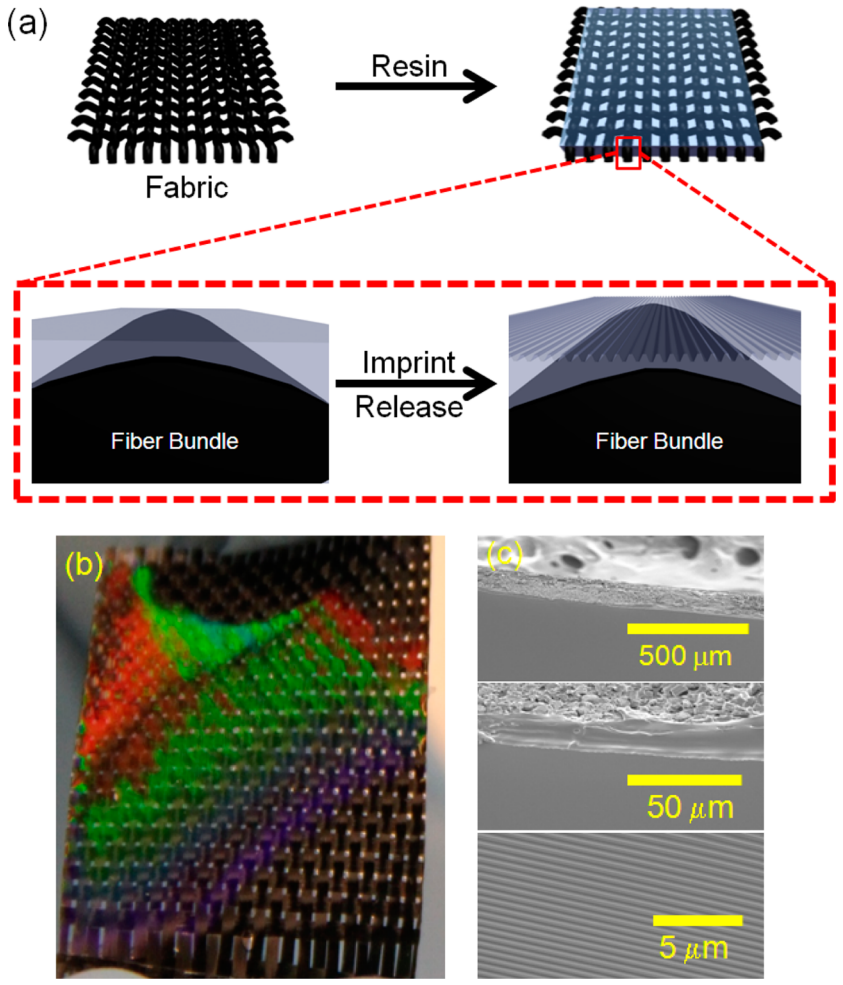

Figure 1. (a) Schematic of the fabrication of a patterned fiber composite. (b) Picture of a patterned carbon fiber/x-PDMS composite. (c) Cross-section SEM images of a Carbon Fiber/x-PDMS composite (top), a more magnified image of the resin/fiber interface (middle) and the imprinted 750 nm gratings.

EXPERIMENTAL SECTION

Materials. Norland Optical Adhesive 63 (NOA 63) was purchased from Norland Optical. Sylgard 184 PDMS (x-PDMS) prepolymer and cross-linker were purchased from Dow Corning. Nylon fabric was purchased from Jo-Ann Fabric and Crafts. Plain weave 1-k carbon fiber, unidirectional 12k carbon fiber, glass fiber (E-glass), and Kevlar-Carbon fiber fabrics were purchased from Composite Envisions. F-15 Polyurethane resin was purchased from B.J.B Enterprises. Whatman filter paper (high cellulose paper) was purchased from Fisher Scientific. Polycarbonate grating masters were created from literature.[35] Poly(ethylene-co-tetrafluoroethylene) (ETFE) was generously provided by Saint-Gobain.

Instrumentation. Atomic force microscopy (AFM) was performed on a Digital Instruments Nanoscope III in tapping mode under ambient conditions. Scanning electron microscopy (SEM) was performed on a FEI Magellan FE-SEM. Mechanical testing was performed on an Instron 5500R.

Fabrication of Molds. Rectangular line patterns formed on the x-PDMS and polyurethane resins were created by using a mold fabricated according to literature procedure.[35] Briefly, a commercially available digital video disk (DVD-R) was separated in half and the patterned edge was immediately washed with copious amounts of isopropanol to remove the organic ink. After drying, AFM was performed to confirm the removal of the organic ink and the size dimensions of the lines. For Norland Optical patterning, a daughter x-PDMS mold was first created by pouring degassed Sylgard 184 prepolymer and cross-linker (10:1 prepolymer-cross-linker) over the polycarbonate master and then was allowed to sit for 15 min at room temperature to ensure the diffusion of prepolymer and cross-linker into the patterns. The total thickness of the x-PDMS replicas was approximately 1 cm. Next, the uncured Sylgard 184 was placed in an oven for approximately 12 h at 70 °C to ensure the Sylgard 184 was cured. Test pattern features, (Figure 2) were fabricated from an ETFE daughter mold that was formed from thermally imprinting from a silicon master mold. x-PDMS granddaughter molds of the test patterns were formed in the same manner as the polycarbonate molds.

Imprint Lithographic Patterning on Fabrics. Using tape, the fabrics were attached to a sheet of PET to ensure the fabric remains flat to minimize thickness variations. Next, a resin was poured over the fabric, and allowed to sit for 1 min to allow the resin to evenly spread over the surface. The polycarbonate mold was directly applied to the surface of the uncured resin. Another sheet of PET was placed on top of the mold and then a slight pressure of 370 Pa (0.054 PSI) was applied to ensure even spreading throughout the composite. In the case of polyurethanes, an x-PDMS daughter mold of the polycarbonate master or an ETFE daughter mold (depending on the pattern) was used and the composite was allowed to sit for 24 h before removing the mold. The x-PDMS composites used the polycarbonate master or ETFE daughter mold directly (depending on the pattern) and cured for 72 h at room temperature, and then cured in an oven for 15 min at 70 °C. Room temperature cures were preferable because of the thermal expansion coefficient mismatch between the resins and carbon fiber. For NOA 63 composites, NOA 63 was poured into an x-PDMS daughter polycarbonate mold or granddaughter test pattern mold and exposed under UV (λ = 365 nm) for 15 min, until the pattern was

dx.doi.org/10.1021/am3017812 | ACS Appl. Mater. Interfaces 2012, 4, 6640−6645

completely solidified. Next, the same mold was removed from the cured NOA 63 film. Uncured NOA 63 was then poured on a fabric, spread, and then the x-PDMS mold that was just used was placed on top of the uncured resin and exposed to UV light. After 15 min, the samples were turned over and cured for an additional 15 min to ensure that the backside of the sample was completely cured.

Mechanical Testing of Fabrics. Bending modulus was measured in a three-point bend configuration (span length = 1.92 cm) where the sample was 4 cm in length, 1.2 cm wide, and had various thicknesses (ranging from 0.1 to 2 mm) depending on the fabric used. The sample was cycled five times at a rate of 1 mm/min to a displacement of 1 mm. Tensile modulus was measured under uniaxial extension. The substrates and composites were cut into a dog bone geometry with a length of 2.6 cm and a width of 0.46 cm and extended at a rate of 1 mm/min until failure.

Cyclic Testing of Fabrics. Rectangular samples (1.2 cm wide × 6 cm long) were cut and taped in between polycarbonate clamps. One side of the fabric composite was clamped to a fixed support and the other end was clamped to a Black & Decker JS660 Orbital Jig Saw. Samples of x-PDMS, PET, and plain weave carbon fiber-x-PDMS composite were evaluated in the cyclic testing. Each sample was subjected to 5000 bending cycles in which the patterned features were under compression, then flipped upside down and an additional 5000 cycles were performed with the features under extension; both loadings were performed at an approximate frequency of 10 Hz, controlled by adjusting the voltage applied to the apparatus

RESULTS AND DISCUSSION

The scope of this study was to demonstrate the ability and advantages of fabrics as a substrate and to understand the materials properties of fabric composites in order to create tunable composites for use as flexible substrates. Inspired by previous work by our team, we aimed to further evaluate the mechanism in which these composites can be very resistant to tensile forces but maintain high flexibility.[36] Our method of creating these fabric composites is described in Figure 1a, and allows for surface patterning via imprint lithography. By imprinting directly into the resin and curing, stable patterns are formed without the need to account for surface instabilities (Figure 1b), unlike many polymer substrates where surface modification is required to provide stable coatings.[9] The dimensions of the line pattern mold for our sample was measured by AFM and had a line width of 400 nm with a periodicity (λ) of 750 nm, a height of 150 nm. After imprinting, we found, λ remained the same at 750 nm; however the line width was reduced to 350 nm, Figure 1c. The residual layer of x-PDMS underneath the patterned face is 38 μm ± 18 μm. An SEM image of the fabric composite cross section (Figure 1c) illustrates the penetration of the resin through the fabric and the resulting line pattern formed on the surface. Imprint lithography can be used for the rapid replication of features[37] and fabrics can in principle be easily scaled to large volumes in roll-to-roll fabrication processes. Furthermore, this patterning technique can be extended to a number of fabrics and resins, shown in Figure 2. x-PDMS and polyurethane are two examples of thermally curable materials that can be used with various organic and inorganic fabrics (Figure 2a–f). The formation of a planar substrate is not limited to thermally cured resins; UV curable resins such as Norland Optical can also be utilized (Figure 2g).

To test the stability of the patterned lines under mechanical deformation, we cycled the composite to a bending radius of 3.1 mm through a rapid deformation (10 Hz) over 10 000 testing cycles (see Figure S2 in the Supporting Informastion). SEM micrographs of the sample before and after the cyclic

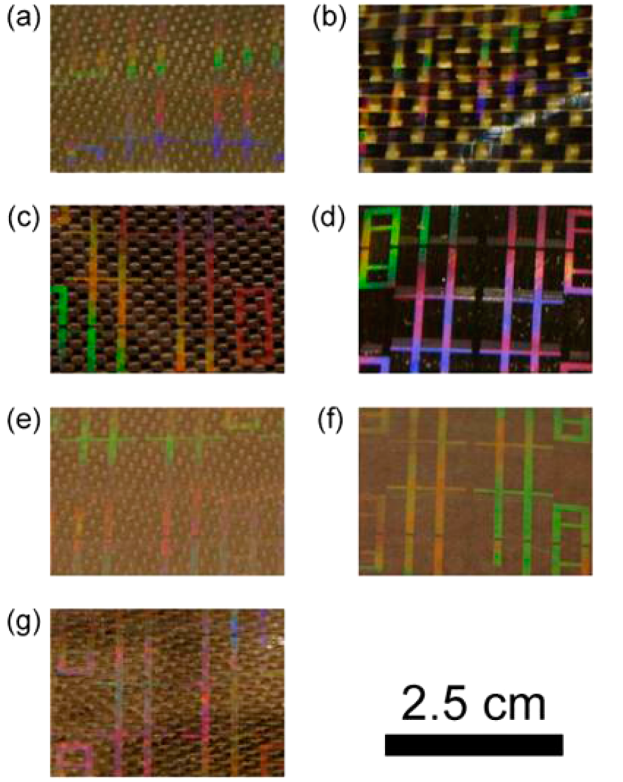

Figure 2. Macroscopic photographs of some of the fabrics and resins that can be implemented: (a) E-glass/x-PDMS, (b) Kevlar-carbon fiber/x-PDMS, (c) plain weave carbon fiber/x-PDMS, (d) Nylon/x-PDMS, (e) E-glass/polyurethane, (f) cellulose paper/x-PDMS, (g) E-glass/Norland Optical 63.

testing show no apparent change in the size or shape of the patterns after testing (Figure 3). Although the sample was bent to a small radius (~3 mm), the maximum strain imposed on the patterned features was only 5.7% because of this samples thickness (360 μm), which is well within the elastic limits of x-PDMS.[15,22] Testing the mechanical properties of free-standing samples of x-PDMS with comparable thicknesses was not possible due to extensive sagging and self-adhesion in the flexure test. Furthermore, the features on the patterned composite did not change regardless if the applied strain was compressive or extensional.

Next, we compared the fabric composite mechanical properties to other commonly used materials, such as cellulose paper, x-PDMS and PET, by subjecting them to tensile and bending strains (see Figure 4). The tensile modulus (E_T) of the samples was determined from a uniaxial extension test and measuring the slope of the stress–strain data. The non-composite x-PDMS (average thickness = 1.75 mm) and PET (average thickness =0.12 mm) substrates were tested and their tensile properties were commensurate with previously reported values with a tensile modulus of 1.2 MPa and 3.7 GPa, respectively.[6,7,13,15,38] Incorporation of x-PDMS into cellulose-paper caused a reduction in the tensile modulus of the sample from 1.1 GPa in cellulose-paper (average thickness = 0.18 mm) to 0.8 GPa in the cellulose-x-PDMS composite (43% vol. paper, average thickness = 0.24 mm). For composites with non-ordered microstructures (e.g., cellulose-paper/x-PDMS) the modulus of the composite (E_c) generally followed the rule of mixtures[39]

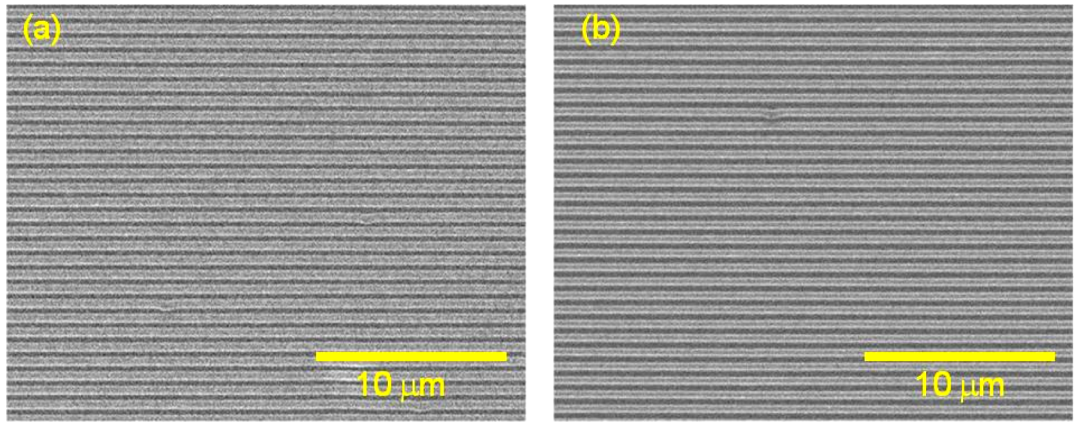

Figure 3. (a) SEM image of a plain weave carbon fiber/x-PDMS composite before cyclic testing; (b) SEM image of same sample after cyclic testing for 10 000 cycles at 10 Hz frequency.

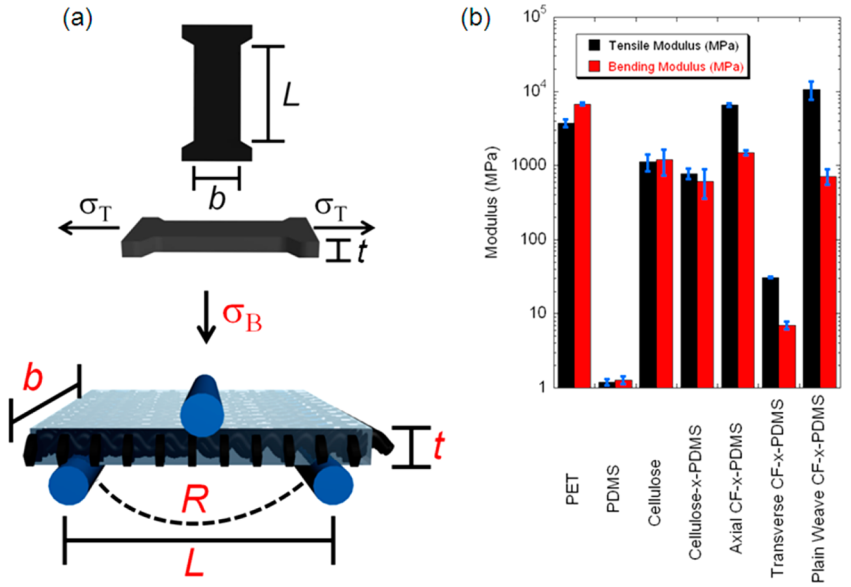

Figure 4. (a) Schematic of the tensile and bending tests and the relevant geometric parameters in those mechanical tests; (b) corresponding tensile and bending moduli for the composites and samples tested.

$$E_C = E_F f + E_R(1 - f) \quad (1)$$

where f is the volume fraction of the fibers and E_F and E_R are the modulus of the fiber and resin, respectively. Accordingly, by embedding cellulose paper in a lower modulus material like x-PDMS, the modulus of the composite is reduced.

For composites with ordered microstructures, such as those created with woven fabrics, anisotropic mechanical properties are expected. The carbon fiber fabrics are composed of 7 μm fibers assembled into bundles which are elliptical in shape. The plain weave fabric bundles are approximately 0.5 mm and 0.06 mm and the unidirectional fabric bundles are approximately 1.95 and 0.625 mm, for the major and minor axes, respectively. A unidirectional carbon fiber/x-PDMS substrate (composite thickness = 0.45 mm, 22 vol % carbon fiber) was tested in two directions to examine the in-plane anisotropy. In the first case, the fibers were oriented orthogonal (transverse) to the pulling and in the second case, the fibers were oriented parallel (axial) to the pulling direction. Straining the composite in the transverse direction distributes the stress between the matrix and the fibers, causing the deformation to primarily occur in the soft x-PDMS matrix.[39] This allows the composite to deform easily, similar to x-PDMS, with a tensile modulus of 32.9 MPa. When the sample was strained axially, the tensile modulus was 6.5 GPa. The significantly higher modulus is due to the fact that the fiber and resin go into a state of equal strain.[39] Since there is a large modulus mismatch ($E_F \gg E_R$), the majority of the stress is supported by the fiber. An even higher tensile modulus is obtained in the plain weave carbon fiber composite (composite thickness = 0.24 mm, 34 vol % carbon fiber) with a modulus of 10.5 GPa. Here, the weave pattern helps to reinforce the fabric against tensile strain.[40] By measuring the tensile modulus, we gained an understanding of the energy density that is required to stretch these composites. To guide material design, we wanted to contrast this energy storage to the energy required to deform the same volume in a bending geometry.

The composite bending moduli (E_B) of the materials were determined using a linear elastic relationship for a simply supported rectangular beam with the load concentrated in the center as

$$E_B = \frac{kL^3}{4bt^3} \quad (2)$$

dx.doi.org/10.1021/am3017812 | ACS Appl. Mater. Interfaces 2012, 4, 6640−6645

where L is the length of the span, b is the width of the sample, t is the thickness of the sample, and k is the experimentally determined bending stiffness of the sample. PET had the highest bending modulus (6.8 GPa), whereas x-PDMS had the lowest bending modulus (1.3 MPa), which is similar to the bulk modulus of x-PDMS. Cellulose paper/x-PDMS composite modulus (0.6 GPa) was lower than pure cellulose (1.2 GPa), again due to the incorporation of a lower modulus matrix. Similar to the tensile testing, the modulus of the carbon fiber composites was dependent on the direction of the fibers with respect to the orientation of the span length. When the composite was bent in the transverse direction with respect to the fibers, the matrix properties dominated the bending behavior, and the modulus (7 MPa) approached that of x-PDMS. However, when the fibers were aligned axially to the span length, the bending stiffness was raised substantially and the unidirectional carbon fiber exhibited a much higher modulus at 1.5 GPa. The plain weave carbon fiber fabric had a relatively high bending modulus (0.7 GPa); however, this value is more than an order of magnitude lower than its tensile modulus (10.5 GPa).

By understanding the differences in the moduli for tension and flexure, we can implement these properties in order to design materials for appropriate flexibility. In Figure 5, the ratio

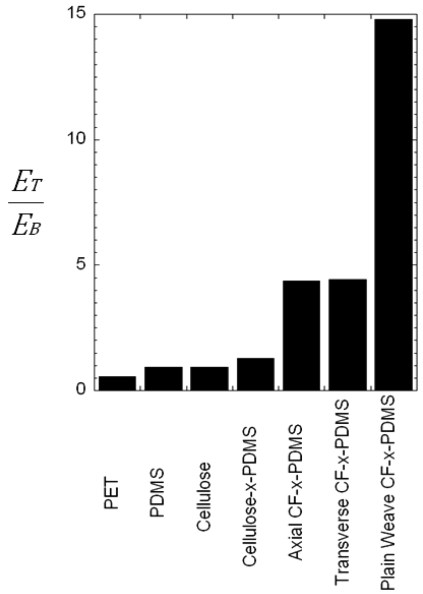

Figure 5. Graph of the ratio of the tensile and bending modulus of the materials tested.

of the tensile modulus to the bending modulus is shown for the composites and materials tested. As expected, x-PDMS and PET approach unity as these are homogeneous materials with no reinforcement or other material affecting the anisotropy of the film. For these types of materials, the bending flexibility comes at the cost of reducing the modulus of the material or keeping a very thin geometry. Both cellulose paper and cellulose paper/x-PDMS also exhibited a ratio that approached unity, which was also expected because the fibrous network was not an ordered microstructure like the other fabric materials. The plain weave carbon fiber exhibited the largest tensile to bending ratio of 14.8, which is a combination of several factors of the composite. Having a matrix with a much lower modulus is crucial for the fiber composite to retain this high difference of stretching to bending. The tensile strain is limited by the stiffer component of the composite when the sample is strained axially. However, in bending, the composite bending modulus is not only a property of modulus mismatch and relative volume fraction, but also the position of the components. In particular, the position of components relative to the neutral axis is a factor in determining bending resistance. The neutral axis for our composites is determined by a relationship

$$E_F \int_{A_F} y dA + E_R \int_{A_R} y dA = 0 \quad (3)$$

where y is the distance of the centroid of the material to the neutral axis of the composite, A_F and A_R are the cross-sectional area of the fiber and the resin, respectively. In our composites, the neutral axis is centered on the middle of the fabric. When the composite is in flexure, the fibers are subjected to the least amount of strain and the matrix will have a larger strain. The greater strain is therefore present in the lower modulus x-PDMS, thus requiring little energy to bend to a given radius of curvature. This allows substrates to possess a higher thickness, yet maintain similar flexibility.

The anisotropy and direction of the fabric also allows for stiffness control in the plane of the substrate.[41,42] Because of the symmetry of the plain weave carbon fiber, the mechanical properties are symmetric within the plane of the fabric. The asymmetric weave pattern (i.e., unidirectional fibers) allows these properties to be different within the plane of the fabric, depending on the alignment of the fibers.[41,42] For the unidirectional carbon fiber composite, there was a substantial difference between the modulus when the composite was strained axially versus transversely relative to the fiber direction. Therefore, if the substrate needs to accommodate strain in one direction of the plane, it can easily be tailored to do so while strongly resisting in the other direction within the same plane. This control of the tensile stress distribution of the composite within the plane is not available in homogeneous planar substrates.

CONCLUSIONS

We have described a versatile and facile method for producing patterned, flexible composite substrates. By using imprint lithography, patterning is incorporated directly into the composite fabrication step, eliminating the need for planarization required in conventional flat substrates. These 400 nm patterns are mechanically stable after 10 000 rapid deformation cycles in both extension and compression. A number of fabric and resin combinations were tested to demonstrate the versatility of this method. Compared to commonly used flexible substrates, these elastomer−fiber composites have superior tensile moduli while still maintaining comparable or superior bending flexibility. By varying the fiber alignment, in-plane anisotropy was observed in the tensile and bending modulus that can be easily adjusted by changing the fabric geometry (unidirectional vs plain weave). We anticipate that this will provide superior attributes in load-bearing applications that are not possible with current materials, such as Sylgard 184 (x-PDMS) and PET. Finally, we have demonstrated the superior in-plane strain resistance that can be achieved while maintaining high flexibility. Fabric reinforcement provides the ability to resist tension strongly, yet allow comparable or superior flexibility given a set geometry. We anticipate these features to provide robust materials for flexible electronics as well as biomedical devices.

■ ASSOCIATED CONTENT

Supporting Information

AFM image of the mold used, pictures of a plain weave carbon fiber-Sylgard 184 composite sample undergoing cyclic testing, and corresponding video of the cyclic testing. This material is free of charge via Internet at http://pubs.acs.org.

■ AUTHOR INFORMATION

Corresponding Author

*E-mail: krcarter@polysci.umass.edu (K.R.C.); crosby@mail.pse.umass.edu (A.J.C.).

Notes

The authors declare no competing financial interest.

■ ACKNOWLEDGMENTS

The authors gratefully acknowledge the University of Massachusetts NSF-Center for Hierarchical Manufacturing (NSF CMMI-10250 20) for funding on this research, Saint-Gobain for generous provisions of ETFE materials, Dr. Jacob John for assistance with ETFE molds, and Louis Raboin for assistance on the SEM images.

■ REFERENCES

(1) Nomura, K.; Ohta, H.; Takagi, A.; Kamiya, T.; Hirano, M.; Hosono, H. *Nature* **2004**, *432* (7016), 488−492.
(2) Sekitani, T.; Iba, S.; Kato, Y.; Noguchi, Y.; Someya, T.; Sakurai, T. *Appl. Phys. Lett.* **2005**, *87* (17), 173502.
(3) Han, L.; Song, K.; Mandlik, P.; Wagner, S. *Appl. Phys. Lett.* **2010**, *96* (4), 042111.
(4) Wagner, S.; Bauer, S. *MRS Bull.* **2012**, *37* (3), 207−217.
(5) Kim, E. H.; Yang, C. W.; Park, J. W. *J. Appl. Phys.* **2012**, *111* (9), 8.
(6) Zardetto, V.; Brown, T. M.; Reale, A.; Di Carlo, A. *J. Polym. Sci., Part B: Polym. Phys.* **2011**, *49* (9), 638−648.
(7) Alzoubi, K.; Hamasha, M. M.; Lu, S. S.; Sammakia, B. *J. Disp. Technol.* **2011**, *7* (11), 593−600.
(8) Sekitani, T.; Someya, T. *Adv. Mater.* **2010**, *22* (20), 2228−2246.
(9) Yang, C. W.; Park, J. W. *Surf. Coat. Technol.* **2010**, *204* (16−17), 2761−2766.
(10) MacDonald, W. A.; Looney, M. K.; MacKerron, D.; Eveson, R.; Adam, R.; Hashimoto, K.; Rakos, K. *J. Soc. Inf. Disp.* **2007**, *15* (12), 1075−1083.
(11) Krebs, F. C. *Org. Electron.* **2009**, *10* (5), 761−768.
(12) Krebs, F. C.; Gevorgyan, S. A.; Alstrup, J. *J. Mater. Chem.* **2009**, *19* (30), 5442−5451.
(13) van den Brand, J.; Kusters, R.; Barink, M.; Dietzel, A. *Microelectron. Eng.* **2010**, *87* (10), 1861−1867.
(14) Kumar, A.; Biebuyck, H. A.; Whitesides, G. M. *Langmuir* **1994**, *10* (5), 1498−1511.
(15) Mata, A.; Fleischman, A. J.; Roy, S. *Biomed. Microdevices* **2005**, *7* (4), 281−293.
(16) Melzer, M.; Makarov, D.; Calvimontes, A.; Karnaushenko, D.; Baunack, S.; Kaltofen, R.; Mei, Y. F.; Schmidt, O. G. *Nano Lett.* **2011**, *11* (6), 2522−2526.
(17) Akter, T.; Joseph, J.; Kim, W. S. *IEEE Electron Device Lett.* **2012**, *33* (6), 902−904.
(18) Akter, T.; Kim, W. S. *ACS Appl. Mater. Interfaces* **2012**, *4* (4), 1855−1859.
(19) Rogers, J. A.; Bao, Z.; Baldwin, K.; Dodabalapur, A.; Crone, B.; Raju, V. R.; Kuck, V.; Katz, H.; Amundson, K.; Ewing, J.; Drzaic, P. *Proc. Natl. Acad. Sci. U.S.A.* **2001**, *98* (9), 4835−4840.
(20) Kim, D. H.; Ahn, J. H.; Choi, W. M.; Kim, H. S.; Kim, T. H.; Song, J. Z.; Huang, Y. G. Y.; Liu, Z. J.; Lu, C.; Rogers, J. A. *Science* **2008**, *320* (5875), 507−511.
(21) Kim, D. H.; Song, J. Z.; Choi, W. M.; Kim, H. S.; Kim, R. H.; Liu, Z. J.; Huang, Y. Y.; Hwang, K. C.; Zhang, Y. W.; Rogers, J. A. *Proc. Natl. Acad. Sci. U.S.A.* **2008**, *105* (48), 18675−18680.
(22) Kim, D. H.; Lu, N. S.; Ghaffari, R.; Kim, Y. S.; Lee, S. P.; Xu, L. Z.; Wu, J. A.; Kim, R. H.; Song, J. Z.; Liu, Z. J.; Viventi, J.; de Graff, B.; Elolampi, B.; Mansour, M.; Slepian, M. J.; Hwang, S.; Moss, J. D.; Won, S. M.; Huang, Y. G.; Litt, B.; Rogers, J. A. *Nat. Mater.* **2011**, *10* (4), 316−323.
(23) Jung, I. W.; Xiao, J. L.; Malyarchuk, V.; Lu, C. F.; Li, M.; Liu, Z. J.; Yoon, J.; Huang, Y. G.; Rogers, J. A. *Proc. Natl. Acad. Sci. U.S.A.* **2011**, *108* (5), 1788−1793.
(24) Sekitani, T.; Zschieschang, U.; Klauk, H.; Someya, T. *Nat. Mater.* **2010**, *9* (12), 1015−1022.
(25) Kim, D. H.; Lu, N. S.; Ma, R.; Kim, Y. S.; Kim, R. H.; Wang, S. D.; Wu, J.; Won, S. M.; Tao, H.; Islam, A.; Yu, K. J.; Kim, T. I.; Chowdhury, R.; Ying, M.; Xu, L. Z.; Li, M.; Chung, H. J.; Keum, H.; McCormick, M.; Liu, P.; Zhang, Y. W.; Omenetto, F. G.; Huang, Y. G.; Coleman, T.; Rogers, J. A. *Science* **2011**, *333* (6044), 838−843.
(26) Martinez, A. W.; Phillips, S. T.; Butte, M. J.; Whitesides, G. M. *Angew. Chem., Int. Ed.* **2007**, *46* (8), 1318−1320.
(27) Martinez, A. W.; Phillips, S. T.; Whitesides, G. M. *Proc. Natl. Acad. Sci. U.S.A.* **2008**, *105* (50), 19606−19611.
(28) Martinez, A. W.; Phillips, S. T.; Wiley, B. J.; Gupta, M.; Whitesides, G. M. *Lab Chip* **2008**, *8* (12), 2146−2150.
(29) Martinez, A. W.; Phillips, S. T.; Carrilho, E.; Thomas, S. W.; Sindi, H.; Whitesides, G. M. *Anal. Chem.* **2008**, *80* (10), 3699−3707.
(30) Carrilho, E.; Phillips, S. T.; Vella, S. J.; Martinez, A. W.; Whitesides, G. M. *Anal. Chem.* **2009**, *81* (15), 5990−5998.
(31) Martinez, R. V.; Fish, C. R.; Chen, X.; Whitesides, G. M. *Adv. Funct. Mater.* **2012**, *22* (7), 1376−1384.
(32) Kim, D. H.; Kim, Y. S.; Wu, J.; Liu, Z. J.; Song, J. Z.; Kim, H. S.; Huang, Y. G. Y.; Hwang, K. C.; Rogers, J. A. *Adv. Mater.* **2009**, *21* (36), 3703−3707.
(33) Sekitani, T.; Noguchi, Y.; Hata, K.; Fukushima, T.; Aida, T.; Someya, T. *Science* **2008**, *321* (5895), 1468−1472.
(34) Jin, J. H.; Ko, J. H.; Yang, S.; Bae, B. S. *Adv. Mater.* **2010**, *22* (40), 4510−4515.
(35) Moran, I. W.; Ell, J. R.; Carter, K. R. *Small* **2011**, *7* (18), 2669−2674.
(36) Bartlett, M. D.; Croll, A. B.; King, D. R.; Paret, B. M.; Irschick, D. J.; Crosby, A. J. *Adv. Mater.* **2012**, *24* (8), 1078−1083.
(37) Ahn, S. H.; Guo, L. J. *ACS Nano* **2009**, *3* (8), 2304−2310.
(38) Wu, J. A.; Li, M.; Chen, W. Q.; Kim, D. H.; Kim, Y. S.; Huang, Y. G.; Hwang, K. C.; Kang, Z.; Rogers, J. A. *Acta Mech. Sin.* **2010**, *26* (6), 881−888.
(39) Matthews, F. L., Rawling, R. D., *Composite Materials: Engineering and Science*; CRC Press: Boca Raton, FL, 1999; p 470.
(40) Dejong, S.; Postle, R. *J. Text. Inst.* **1977**, *68* (11), 350−361.
(41) Khatibzadeh, M.; Piggott, M. R. *Compos. Sci. Technol.* **1996**, *56* (12), 1435−1442.
(42) Khatibzadeh, M.; Piggott, M. R. *Compos. Sci. Technol.* **1996**, *56* (12), 1443−1451.